



Article

Establishment of RNA Interference Genetic Transformation System and Functional Analysis of FlbA Gene in *Leptographium qinlingensis*

Tian Gan , Huanli An , Ming Tang and Hui Chen *

State Key Laboratory for Conservation and Utilization of Subtropical Agro-Bioresources, College of Forestry and Landscape Architecture, South China Agricultural University, Guangzhou 510642, China;

zzm_ahl@stu.scau.edu.cn (H.A.); tangming@scau.edu.cn (M.T.)

* Correspondence: chenhui@scau.edu.cn; Tel.: +86-135-1911-6730

Abstract: *Leptographium qinlingensis* is a pathogenic fungus of *Pinus armandii* that is epidemic in the Qinling Mountains. However, an effective gene interference strategy is needed to characterize the pathogenic genes in this fungus on a functional level. Using the RNA silencing vector pSilent-1 as a template, we established an RNA interference genetic transformation system mediated by *Agrobacterium tumefaciens* GV3101, which is suitable for the gene study for *Leptographium qinlingensis* by homologous recombination and strain interference system screening. The LqFlbA gene was silenced using the RNA interference approach described above, and the resulting transformants displayed various levels of silencing with a gene silencing effectiveness ranging from 41.8% to 91.4%. The LqFlbA-RNAi mutant displayed altered colony morphology, sluggish mycelium growth, and diminished pathogenicity toward the host *P. armandii* in comparison to the wild type. The results indicate that this method provides a useful reverse genetic system for studying the gene function of *L. qinlingensis*, and that LqFlbA plays a crucial role in the growth, development, and pathogenicity of *L. qinlingensis*.

Keywords: *Leptographium qinlingensis*; RNA interference; *Agrobacterium tumefaciens*; FlbA; pathogenicity



Citation: Gan, T.; An, H.; Tang, M.; Chen, H. Establishment of RNA Interference Genetic Transformation System and Functional Analysis of FlbA Gene in *Leptographium qinlingensis*. *Int. J. Mol. Sci.* **2023**, *24*, 13009. <https://doi.org/10.3390/ijms241613009>

Academic Editor: Alessio Mengoni

Received: 15 July 2023

Revised: 17 August 2023

Accepted: 19 August 2023

Published: 21 August 2023



Copyright: © 2023 by the authors. Licensee MDPI, Basel, Switzerland. This article is an open access article distributed under the terms and conditions of the Creative Commons Attribution (CC BY) license (<https://creativecommons.org/licenses/by/4.0/>).

1. Introduction

The *Pinus armandii*, commonly known as Chinese white pine, stands as a native and pioneering coniferous species within the Qinling Mountains of China [1]. It assumes a crucial ecological and societal responsibility in water and soil conservation, thus wielding a significant impact on the local economy and ecology [2]. However, a rapid, widespread decline in Chinese white pine (*P. armandii*) has been brought on by an interaction biological complex (CWPB-Lq complex) that is formed of the Chinese white pine beetle (*Dendroctonus armandi*, CWPB) and the ascomycetes fungus (*Leptographium qinlingensis*, Lq) [3–5]. The activities of *L. qinlingensis* culminate in disruptions of nutrient and water metabolism, eventually leading to the demise of host trees due to the destruction of resin-producing cells and the obstruction of resin canals [6]. Additionally, according to recent research, symbiotic fungi help beetles invade trees by detoxifying the chemical defenses of the trees and providing the insects with nourishment [7–12].

L. qinlingensis belongs to the ophiostomatoid fungi. Given the wealth of biological information available on this pathogenic CWPB-associate, it is the primary target in our current and ongoing genomics work. Li et al. (2012) reported three plant toxins and their activities in metabolites secreted by *L. qinlingensis* [1]. Dai et al. (2015, 2022) systematically studied the phylogenetic development of the CYP450 family genes in *L. qinlingensis* and their detoxification mechanism in overcoming pine defense compounds [13,14]. Furthermore, Dai et al. (2022) delved into the transcriptomic analysis of *L. qinlingensis*, revealing key genes and enzymes participating in terpene tolerance and nutritional utilization [8].

An et al. (2022) explored the intricate connection between the TOR gene and various factors such as carbon sources, nitrogen sources, host nutrients, and host volatiles (monoterpenoids) within *L. qinlingensis* [15]. Gan et al. (2022) reported on the role of RGS family genes in the fungal growth and development of, as well as in overcoming the host chemical resistance of, *L. qinlingensis* [4]. Nevertheless, the verification of gene functions and their contributions to pathogenicity necessitates the generation of mutants (or transformants) of *L. qinlingensis*, wherein the genes of interest are either deleted or modified. The methodologies for gene replacement and modification require tailored optimization for each fungal species, a task that has not yet been accomplished for *L. qinlingensis*.

RNA interference (RNAi) is a simple, quick, precise way of exploring gene function, applied to switching off genes in plants, animals, insects, and many other higher organisms [16]. Notably, RNAi has been successfully employed within numerous fungi [17–23]. Nakayashiki et al. (2005) pioneered the development of a restriction enzyme-based silencing vector, pSilent-1, tailored for RNA silencing investigations in filamentous fungi [18]. Meanwhile, the *Agrobacterium tumefaciens*-mediated transformation (ATMT) system is gaining popularity as an effective insertional mutagenesis method for gene overexpression, gene targeting, and T-DNA insertional mutagenesis in a variety of filamentous fungus [24–26]. In contrast to protoplast-mediated transformation (PMT), ATMT confers a discernible advantage, given its capacity to facilitate the direct exploitation of fungal spores for genetic manipulation, obviating the requisite for protoplasts [27]. Despite its widespread application in various filamentous fungi, the successful implementation of ATMT within the context of *L. qinlingensis* has yet to be realized. The pressing need revolves around establishing a dependable methodology for achieving stable genetic transformation in *L. qinlingensis*, thereby enabling the comprehensive characterization of the functional roles encoded by its virulence genes.

Within filamentous fungi, heterotrimeric G proteins regulate multiple physiological processes by regulating adenylate cyclase and phospholipase activities [28–31]. As a negative regulator of G protein signaling, the G protein signaling regulator (RGS) is involved in many physiological processes such as the growth and development of filamentous fungi. FlbA constitutes the inaugural scrutinized RGS protein within the domain of model filamentous fungi [32]. Extant research has incontrovertibly elucidated the pivotal role of the *FlbA* gene in governing the growth and development of numerous filamentous fungal species [33–35]. In the model fungus *Aspergillus nidulans*, *AnFlbA* regulates germination of conidia and tolerance of environmental stress [36]. The *MoRgs1 (FlbA)* of *Magnaporthe oryzae* controls conidia and appressorium formation [31]. In *Fusarium verticillioides*, *FvFlbA2* has a negative regulation of conidial production [37]. In our previous study, the *FlbA* gene played a role in the growth and pathogenicity of *L. qinlingensis* [4]. In light of its gene functionality and discernible phenotypic alterations, the *FlbA* gene was selected as the designated target for knockdown in the context of this investigation.

In the work reported here, we established a genetic transformation system for *L. qinlingensis* by conjoining *A. tumefaciens*-mediated transformation (ATMT) with RNA interference (RNAi). Through the targeted manipulation of the *LqFlbA* gene, we achieved the generation of transformants characterized by gene silencing, thereby elucidating the influence of *LqFlbA* on fungal growth and pathogenicity. This account stands as the inaugural report detailing the achievement of a successful and stable genetic transformation within this species. Consequently, this accomplishment holds promising implications for the prospective advancement of genetic manipulation in closely related fungal taxa.

2. Results

2.1. Antibiotic Sensitivity of Experimental Strains

Hygromycin B sensitivity in *L. qinlingensis* was evaluated by incubating the isolate on PDA supplemented with various concentrations of hygromycin B (up to 100 µg/mL) at temperatures of 28 °C for 7 days in darkness. Growth was fully suppressed at the hygromycin B concentration of 50 µg/mL (Figure 1A); consequently, this threshold was employed to

select the resistant transformants in the context of ATMT experiments. Meanwhile, varying concentrations (up to 300 $\mu\text{g}/\text{mL}$) of cefotaxime or timentin exhibited no discernible impact on the growth of *L. qinlingensis*. Application of cefotaxime and timentin was undertaken to eliminate *A. tumefaciens* in the elective PDA medium. *A. tumefaciens* GV3101 growth was completely arrested at a cefotaxime concentration of 50 $\mu\text{g}/\text{mL}$ (Figure 1B) and a timentin concentration of 150 $\mu\text{g}/\text{mL}$ (Figure 1C); consequently, these specific concentrations were adopted for the eradication of *A. tumefaciens* in the ATMT experiments.

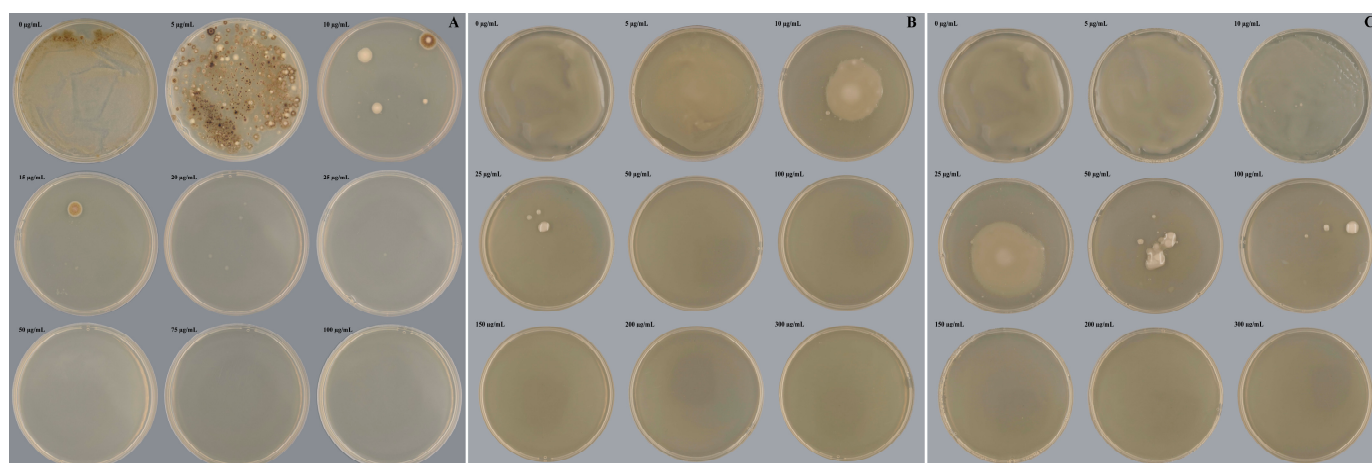


Figure 1. Antibiotic sensitivity of experimental strains. (A) Hygromycin B sensitivity of *L. qinlingensis*; (B) Cefotaxime sensitivity of *A. tumefaciens* GV3101; (C) Timentin sensitivity of *A. tumefaciens* GV3101.

2.2. ATMT of *L. qinlingensis*

The effect of different cocultivation parameters (*A. tumefaciens* and *L. qinlingensis* concentrations, cocultivation duration, temperature, pH of the medium, and acetosyringone concentration) on the transformation efficiency of *L. qinlingensis* was evaluated with the pSilent-1 vector. The transformation rate was determined by calculating the number of transformants obtained under different parameter conditions.

The study on the impact of six different cocultivation temperatures (viz. 25, 26, 27, 28, 29, and 30 $^{\circ}\text{C}$) on the transformation rate showed that higher numbers of transformants were achievable at 28 $^{\circ}\text{C}$ (Figure 2A). Among the tested cocultivation periods (24, 36, 40, 48, 56, and 64 h), a 48 h incubation period was optimal for obtaining a higher yield of transformants (Figure 2B). Lower transformation efficiency was noted with a longer cocultivation period. Among the 7 different pH values (pH 4.4, 4.7, 5.0, 5.3, 5.6, 5.9, and 6.2) of the cocultivation medium evaluated, higher numbers of transformants were noted at pH 5.0–5.6 (Figure 2C). Cocultivation performed with 200 μM acetosyringone yielded the highest transformation rate compared to the other tested concentrations (50, 100, 300, and 400 μM). A decrease in the number of transformants was noted with an increase in the acetosyringone concentration (Figure 2D). Among the tested cell concentrations of *Agrobacterium* ($\text{OD}_{600} = 0.3, 0.4, 0.5, 0.6, 0.7, \text{ and } 0.8$) and conidial suspension ($10^4, 10^5, 10^6, 10^7, \text{ and } 10^8$ spores/mL), *Agrobacterium* ($\text{OD}_{600} = 0.5\text{--}0.6$) and conidial suspension (1×10^6 spores/mL), respectively, were found to be ideal for generating higher numbers of transformants (Figure 2E,F).

Collectively, the transformation efficiency increased using the *Agrobacterium* ($\text{OD}_{600} = 0.5\text{--}0.6$) and conidial suspension (1×10^6 spores/mL) in the cocultivation medium with a pH value of 5.0–5.6. The transformation should occur at 28 $^{\circ}\text{C}$ in the presence of 200 μM acetosyringone for no longer than 48 h to yield a high transformation efficiency.

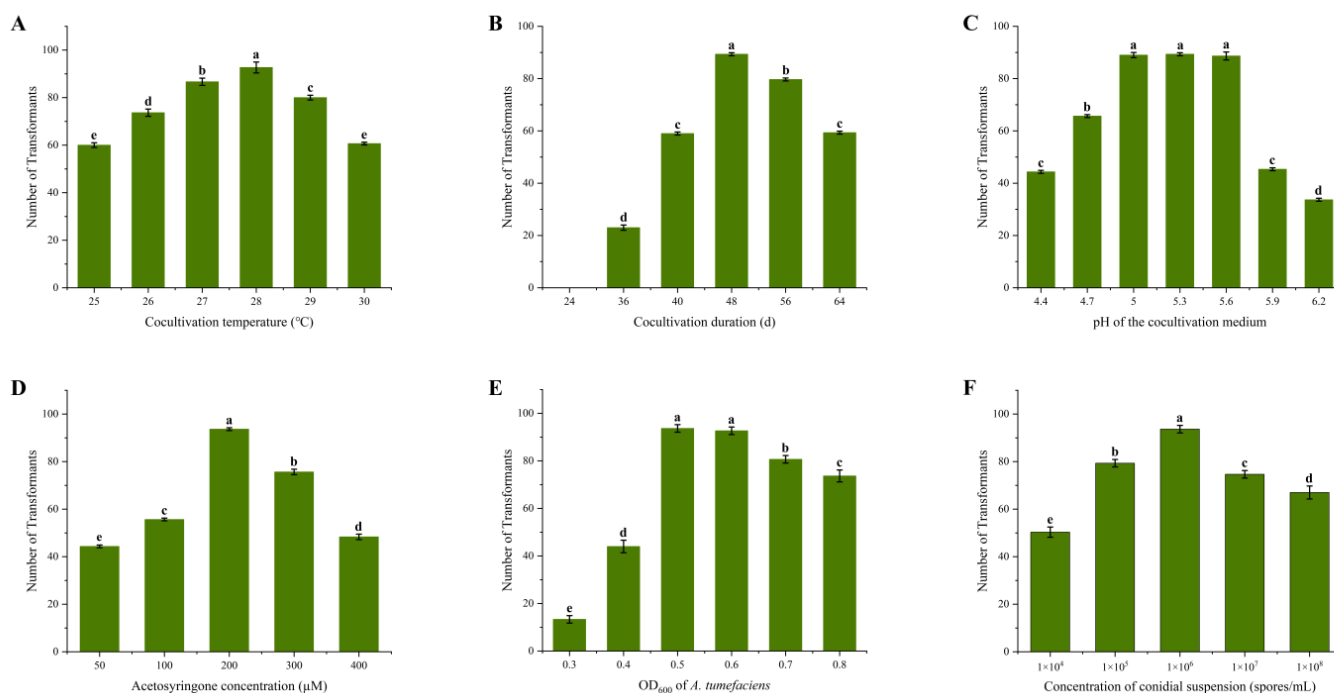


Figure 2. The effects of different cocultivation parameters on ATMT of *L. qinlingensis*. (A) Cocultivation temperature; (B) Cocultivation duration; (C) pH of the cocultivation medium; (D) Acetosyringone concentration; (E) The concentration of *A. tumefaciens* GV3101; (F) The conidia concentration of *L. qinlingensis*. The values are the means \pm SE of three independent experiments. Error bars represent standard deviation from repeats. Different letters indicate a significant difference between different treatments ($p < 0.05$).

2.3. Confirmation of Transformants

To validate the accurate gene integration within the transformants, we selected three positive transformants (designated as LqFlbA-RNAi-1, LqFlbA-RNAi-2, and LqFlbA-RNAi-3), and juxtaposed them with a transformant harboring the vacant vector (referred to as LqFlbA-EV) following a series of five consecutive screening iterations. By employing specific primers (Hyg-F/R, Test-F/R) in PCR analyses, we successfully verified the presence of recombinant fragments and the hygromycin resistance (*Hyg*) gene. All three transformants, alongside LqFlbA-EV, exhibited the anticipated amplicons, namely a band corresponding to the recombinant fragment (484 bp) and a *Hyg* band (1040 bp), while displaying no bands for the wild type (WT). PCR products of the amplified *Hyg* gene were sequenced correctly (Figure 3A). Subsequent sequencing of PCR products using the Test-F/R primers revealed the presence of recombinant fragments in all three positive transformants, while no hairpin structures were detected in LqFlbA-EV.

To assess the efficacy of target gene silencing in the transformants, we employed specific primers (FlbA-F/R) and performed quantitative real-time PCR (qRT-PCR) to quantify the relative expression levels of the target genes across the three transformants and LqFlbA-EV. Compared with WT, the expression level of the *FlbA* gene was not significantly changed in LqFlbA-EV, while the *FlbA* gene expression level was significantly reduced in the three transformants, with gene silencing efficiency of 41.8%, 87.7%, and 91.4%, respectively (Figure 3B).

2.4. LqFlbA Is Required for the Growth and Reproduction of *L. qinlingensis*

To ensure consistent medium conditions, LqFlbA-EV was used as a control to compare hyphal growth after *LqFlbA* gene silencing. We detected that *FlbA* gene silencing caused the premature termination of colony growth in *L. qinlingensis* (Figure 4A). LqFlbA-RNAi-1, LqFlbA-RNAi-2, and LqFlbA-RNAi-3 stopped growing on the 25th, 20th, and 20th days,

respectively, with colony areas of only 56.9%, 33.2%, and 27.2% of the control. Altogether, these findings reveal that the more efficient *FlbA* gene silencing, the lower the growth rate of the transformants and the more inhibited the colony growth.

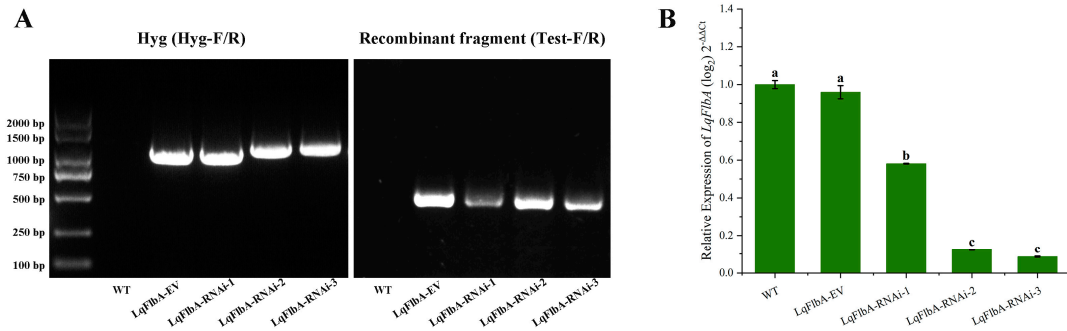


Figure 3. Molecular characterization of *FlbA* gene silencing transformants. (A) PCR amplification of recombinant fragment (484 bp), Hyg (1040 bp) using primers indicated in a from WT, LqFlbA-EV, and LqFlbA-RNAi transformants. (B) Transcriptional levels of LqFlbA in WT, LqFlbA-EV, and LqFlbA-RNAi transformants by real-time qRT-PCR analysis. Different letters indicate a significant difference between different treatments ($p < 0.05$).

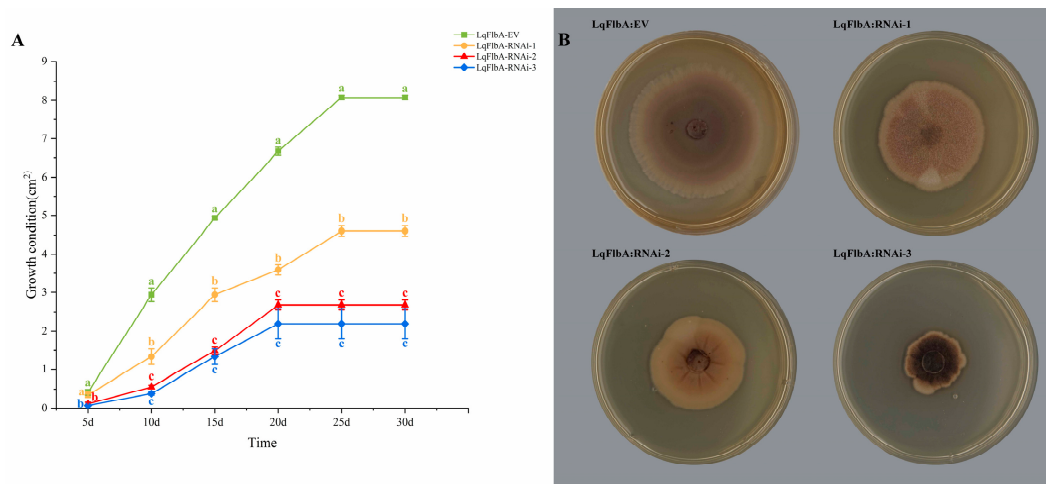


Figure 4. Effect of *LqFlbA* silencing on the growth and reproduction of *L. qinlingensis*. (A) Growth rate of LqFlbA-EV and 3 RNAi transformants. The growth condition was obtained by calculating the area of the colony. The results represent the mean \pm SE of three independent experiments. Different letters indicate a significant difference between different strains ($p < 0.05$). (B) Phenotypes of LqFlbA-EV and 3 RNAi transformants on PDA plates (added 50 μ g/mL hygromycin B).

Compared with the control (LqFlbA-EV), the colony morphology of the three RNAi transformants changed (Figure 4B). The mycelium of LqFlbA-RNAi-3 has more melanin deposition and a darker colony color. The mycelium growth of LqFlbA-RNAi-2 accumulates longitudinally, and the colonies exhibit longitudinal ridges that diverge from the center to the surrounding areas. LqFlbA-RNAi-1 showed white powdery hyphae free from the PDA plate, with uneven colony coloring. None of the three RNAi transformants colonies produced ring-like discoloration.

2.5. Knockdown of *LqFlbA* Results in Diminished Pathogenicity of *L. qinlingensis*

To ascertain whether *FlbA* plays a pivotal role in the colonization and infection processes of pine trees, LqFlbA-RNAi-3 (exhibiting the highest silencing efficiency), the wild-type strain, and non-inoculated agar (serving as a control) were chosen for inoculation onto two-year-old *P. armandii* seedlings. Spot length was measured at 15 days and the

fungi on the spot were reisolated and identified. The outcomes unequivocally revealed that the knockdown of *LqFlbA* led to a discernible reduction in the pathogenic potential of *L. qinlingensis* (Figure 5). At the culmination of a 15-day interval, the wild-type strain elicited a brown-hued lesion, measuring approximately 1 cm in length (averaged from three independent experiments), within the phloem and sapwood. In contrast, *LqFlbA*-RNAi-3 and the agar control treatments elicited a notably subdued response. Subsequent to a 30-day period, seedlings inoculated with the wild-type strains displayed a yellowing of their needles, accompanied by an approximately 1.5 cm long disease spot. Conversely, pine trees subjected to *LqFlbA*-RNAi-3 and the control exhibited robust health, with negligible discernible reactions at the inoculation site. Notably, both the wild-type and transformant variants were successfully isolated from the periphery of the inoculation site.

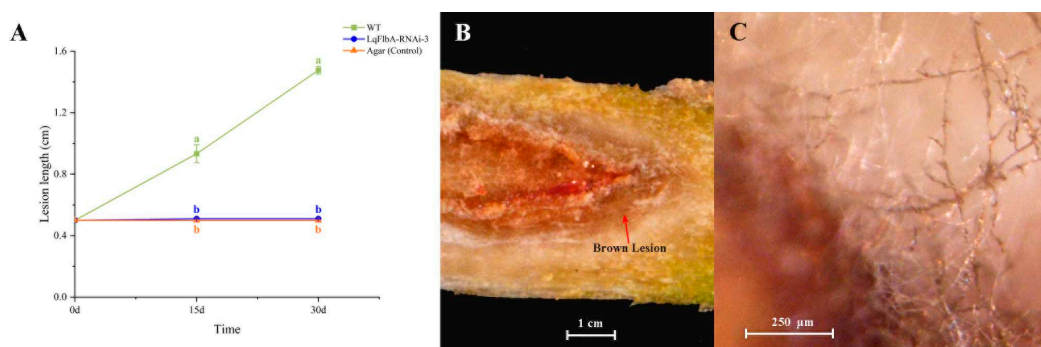


Figure 5. Effect of the *LqFlbA* on the pathogenicity of *L. qinlingensis*. (A) Disease spot length on *P. armandii* seedlings inoculated with WT and RNAi transformants. The wild type successfully colonized and grew on pine seedlings, while the *LqFlbA*-RNAi-3 and agar control did not produce a significant reaction. Each treatment was repeated three times with new sapling and fungal for each replicate. Different letters indicate a significant difference between different strains ($p < 0.05$). (B) The wild type induced a brown lesion in the phloem and sapwood. (C) Hyphae of *L. qinlingensis* growing near the diseased spot tissue.

3. Discussion

Functional assessments of target genes in filamentous fungi conventionally necessitate the establishment of a robust and efficient genetic transformation system [38,39]. RNA interference (RNAi) is a sequence-specific post-transcriptional gene silencing phenomenon and has been used successfully for gene knockdown in filamentous fungi [18,40]. A central advantage inherent to RNAi resides in its non-invasive alteration of the genomic structure, unlike gene knockout methodologies, thus ensuring that the gene expression remains partially sustained rather than being entirely abrogated [41]. Nakayashiki et al. (2005) developed a restriction enzyme-based silencing vector, pSilent-1, for RNA silencing studies in filamentous fungi [18]. The pSilent-1 vector has been effectively used to investigate the role of genes in a variety of filamentous fungi. In *Metarhizium anisopliae*, pSilent-1 plasmid was used interfered with the *swnk* gene of the WT strain [42]. Using the pSilent-1 vector, the *chr-1* gene was suppressed in *Neurospora crassa*, resulting in transformants that displayed resistance to chromate and reduced accumulation of chromium [43]. Scindiya et al. employed the RNA interference (RNAi) methodology via the pSilent-1 vector to systematically investigate the functional attributes of pathogenicity-associated genes (PKS1, GT, and SNF1), thereby elucidating their respective contributions to virulence within *Colletotrichum falcatum* [44,45]. The *A. tumefaciens*-mediated transformation (ATMT) method, characterized by enhanced stability and efficiency, surpasses conventional transformation methodologies in its applicability to fungal transformation processes [46,47]. The ATMT method has been applied to many ascomycetes [48–53]. To further validate the selected pathogenicity gene, attempts were made to standardize the RNAi-based approach during *L. qinlingensis* pathogenesis. Since our earlier study confirmed that *FlbA* plays a role in

the growth and pathogenicity of *L. qinlingensis* [4], functional analysis of the *FlbA* gene has been selected for the RNAi approach using the fungal transformation vector pSilent-1 through *Agrobacterium*-mediated transformation (ATMT) and achieved knockdown of the target genes.

Many factors affect the ATMT efficiency, e.g., the type of starting fungal material (protoplast, spore, and hypha), bacterial and fungal cell concentrations, temperature, length of co-incubation, and concentration of acetosyringone, which is a plant metabolite released from wounded roots that enhances *A. tumefaciens* transformation [54,55]. The observed variations in transformation conditions can be attributed to fungal biodiversity. In this study, we investigated the factors that impact the efficiency of ATMT for *L. qinlingensis* (Figures 2 and 3). Our findings revealed that *L. qinlingensis* is highly sensitive to hygromycin B. In comparison to other types of ascomycetes fungi, a lower concentration of hygromycin B (50 µg/mL) was sufficient to impede the growth of *L. qinlingensis* conidia (Table 1). This revelation holds the potential for strategic utilization in the chemical management of *L. qinlingensis*.

Table 1. Sensitivity to hygromycin B of pathogenic ascomycetes fungi.

Ascomycetes Fungi	Host Tree	Sensitivity to Hygromycin B
<i>L. qinlingensis</i>	<i>P. armandii</i>	50 µg/mL
<i>Neonectria galligena</i>	Broad-leaved tree species	50 µg/mL [56]
<i>Ophiostoma piceae</i>	Coniferous trees	250 µg/mL [57]
<i>Ophiostoma ulmi</i>	Elm	200 µg/mL [58]
<i>Valsa mali</i> var. <i>mali</i> (Vmm)	Apple tree	60 µg/mL [59]
<i>Sphaerulina musiva</i>	<i>Populus trichocarpa</i>	50 µg/mL [60]
<i>Corynespora cassicola</i>	Hevea brasiliensis	100 µg/mL [61]
<i>Monilinia fructicola</i>	Stone and pome fruit	100 µg/mL [62]
<i>Dothistroma septosporum</i>	Coniferous trees	100–200 µg/mL [63]
<i>Raffaelea lauricola</i>	<i>Persea palustris</i> and <i>Persea americana</i>	110 µg/mL [64]

In filamentous fungi, RGS proteins play crucial roles in fundamental biological processes [28,32,65,66]. FlbA is only the second RGS protein to be identified, and plays a central role in attenuating heterotrimeric G-protein-mediated vegetative growth signaling in fungi [36]. In the model filamentous fungus *Aspergillus nidulans*, deletion of the *FlbA* results in the undifferentiated proliferation of hyphal mass and the absence of sexual/asexual sporulation as well as blockage of the mycotoxin sterigmatocystin (ST) production [67–69]. In order to corroborate the *FlbA* gene silencing among the transformants, the mutants underwent scrutiny via qRT-PCR assays for *FlbA* expression in the context of this study. The three transformants exhibited notable disparities, conceivably attributable to the pSilent-1 gene silencing vector. Due to the integrity of the transcriptional unit of target gene hairpin RNA varies in the transformant genome, the gene silencing efficiency varies in the transformants. The transformants were categorized as strongly silenced transformants (0–25%), moderately silenced transformants (50–75%), and non-silenced transformants (75–100%), based on the expression level of the target genes (compared to the wild type) [18]. In this study, LqFlbA-RNAi-2 and LqFlbA-RNAi-3 belonged to strongly silenced transformants, whereas LqFlbA-RNAi-1 belonged to moderately silenced transformants. Due to the intact hairpin structure in the strongly silenced transformants genome and the low risk of transgene loss, strongly silenced transformants were preferentially selected for the subsequent gene function validation. The results of this study showed that there were clear differences in the LqFlbA-RNAi transformants and WT in growth and pathogenicity. Knockdown of *FlbA* reduced the growth and pathogenicity of *L. qinlingensis*. These outcomes robustly corroborate the postulation that the RNAi and ATMT methodologies can effectively facilitate the isolation of functional genes and the identification of pathogenicity-associated genes within *L. qinlingensis*.

In conclusion, we developed an efficient genetic transformation system for *L. qinlingensis*, a bark beetle-vectored fungal pathogen associated with the Chinese white pine. The approach amalgamated *A. tumefaciens*-mediated transformation (ATMT) with RNA interference (RNAi) techniques. The procedure demonstrated notable efficacy, yielding transformants characterized by the *FlbA* gene knockdown within our wild-type *L. qinlingensis* strain. The elucidated genetic transformation system delineated within this study will serve as a pivotal tool for the functional elucidation of genes implicated in the pathogenicity of *L. qinlingensis*, thus facilitating a comprehensive understanding of the mechanisms through which the fungus can bypass or overcome tree defense mechanisms.

4. Materials and Methods

4.1. Strains, Plasmids, and Media

L. qinlingensis (NCBI Taxonomy ID: 717,526) was isolated from *P. armandii* sapwood phloem that had been attacked by the *D. armandi* in the Qinling Mountains and deposited at the College of Forestry and Landscape Architecture, South China Agricultural University (Guangzhou, China). *Escherichia coli* (DH5 α) and *A. tumefaciens* (GV3101) were purchased from Shanghai Weidi Biotechnology Co., Ltd. (Shanghai, China). Plasmid pSlient-1 was purchased from Beijing Jiarui Hengtong Biotechnology Co., Ltd. (Beijing, China).

Potato dextrose agar (PDA) medium (2% glucose, 1.5% agar) was used for the cultivation of *L. qinlingensis*. When screening transformants, appropriate concentrations of antibiotics need to be added to the PDA culture medium. Luria–Bertani (LB) medium (0.5% yeast extract, 1% tryptone, 1% NaCl, solid LB medium with 1.5% agar) was used for the culture of *E. coli* and *A. tumefaciens* GV3101. Induction medium (IM) and co-cultivation medium (CM) were used for fungal transformation and required the addition of 0.2 mol/L acetosyringone (AS) [70].

4.2. Construction of Silencing Vectors

The construction of the gene silencing vector was modified from the method of Zhong et al. [71]. XhoI and ApaI sites on pSlient-1 were selected as cleavage sites for double enzyme digestion, two linearized fragments of pSlient-1 were obtained, and the larger fragments were recovered and stored at $-20\text{ }^{\circ}\text{C}$. The RNA silencing target of the *LqFlbA* gene was designed using DSIR (<http://biodev.extra.cea.fr/DSIR/DSIR.html>, accessed on 15 July 2023), and homologous arms of the XhoI and ApaI cleavage sites were added on both sides of the target. Using the pSlient-1 vector as a template, a fragment containing two reverse-complementary *LqFlbA* silencing targets (called a hairpin region) was amplified and stored at $-20\text{ }^{\circ}\text{C}$. The fusion of the two aforementioned fragments was accomplished using the recombinant enzyme Exnase II (C112-02, Vazyme, Nanjing, China) for the execution of the homologous recombination, followed by the subsequent introduction of the resultant constructs into *E. coli* DH5 α . Positive clones were meticulously chosen for PCR-based identification and subsequent sequencing, ensuring the validation of their accuracy. This rigorous validation procedure was undertaken to attain the conclusive construction of the RNA silencing vector pSlient-1: LqFlbA (Figure 6). The pSlient-1 vector without the hairpin region (called pSlient-1:EV) was used as the control (RNAi empty vector).

4.3. Antibiotic Sensitivity of Experimental Strains

The conidial suspension of *L. qinlingensis* (10^6 /mL, 100 μL) was grown on PDA medium with added different concentrations of hygromycin B (0, 5, 10, 15, 20, 25, 50, 75, and 100 $\mu\text{g}/\text{mL}$), cefotaxime (0, 25, 50, 100, 150, 200, 250, 300, and 350 $\mu\text{g}/\text{mL}$) and timentin (0, 25, 50, 75, 100, 150, 200, 250, and 300 $\mu\text{g}/\text{mL}$), and incubated at $28\text{ }^{\circ}\text{C}$, in darkness, for 7 d to monitor its sensitivity level. Antibiotics were purchased from Sangon Biotech (Shanghai) Co., Ltd. (Shanghai, China).

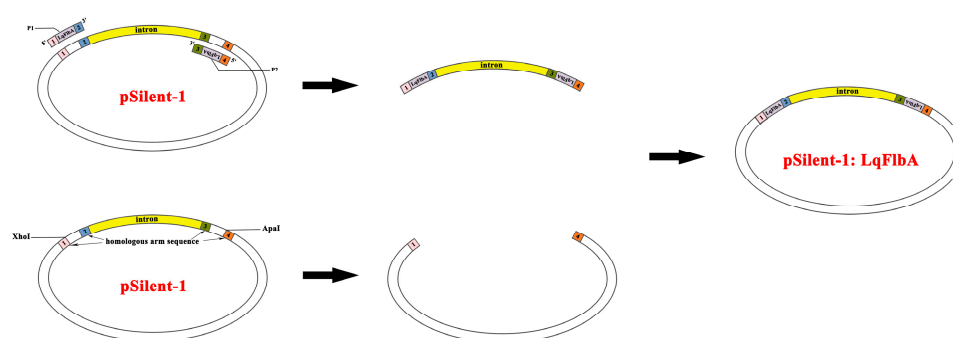


Figure 6. Schematic diagram for constructing silencing vectors. Double-enzyme digestion was performed at the XhoI and ApaI sites to obtain the pSilent-1 vector linearized fragment. A fragment containing one pair of reverse complementary silencing targets was obtained by PCR amplification using pSilent-1 vector as template and P1 and P2 as primers. The RNA silencing vector pSilent-1: LqFlbA was obtained by homologous recombination of the two fragments obtained as described above using the recombinant enzyme Exnase II.

We inoculated *A. tumefaciens* GV3101 containing pSilent-1 (empty vector) into the LB liquid medium and oscillated for 200 r/min. Then, we uniformly coated 100 μ L *A. tumefaciens* GV3101 ($OD_{600} = 0.5\text{--}0.6$) onto the PDA medium with different concentrations of cefotaxime (0, 5, 10, 25, 50, 100, 150, 200, and 300 μ g/mL) and timentin (0, 5, 10, 25, 50, 100, 150, 200, and 300 μ g/mL) added, and incubated it at 28 $^{\circ}$ C, in darkness, for 7 d to monitor its sensitivity level.

4.4. *A. tumefaciens*-Mediated Transformation (ATMT)

We referred to the operating instructions for the method of transferring the RNA silencing vector (pSilent-1: LqFlbA or pSilent-1:EV) into the *A. tumefaciens* GV3101 receptive cells. The GV3101 strain (carrying the RNA silencing vector) was washed 3 times with 1 mL IM liquid medium, and then shaken at 200 r/min until $OD_{600} = 0.5\text{--}0.6$. After 7 days of cultivation on the PDA medium, the *L. qinlingensis* was rinsed with sterile distilled water to yield an asexual spore suspension. The spore suspension was passed through three layers of lens paper to exclude mycelial fragments. Following this, the spores underwent triple rinsing with IM liquid medium. Subsequently, the conidial suspension was adjusted to a concentration of 1×10^6 spores/mL.

A 100 μ L conidial suspension (1×10^6 spores/mL) mixed with a 100 μ L *A. tumefaciens* ($OD_{600} = 0.5\text{--}0.6$) was spread on the 0.45 mm pore nitrocellulose filter laid on the CM plates with the appropriate concentration of acetosyringone (200 μ M), and incubated for 48 h at 28 $^{\circ}$ C. Subsequently, the nitrocellulose filters were transferred onto PDA selective plates containing suitable concentrations of hygromycin B (50 μ g/mL), cefotaxime (50 μ g/mL), and timentin (150 μ g/mL). Upon the anticipated emergence of putative transformants, they were manually isolated and subsequently transferred onto fresh PDA selective plates containing the determined concentration of hygromycin B (50 μ g/mL), as ascertained through the antibiotic sensitivity assay. These isolates were then incubated at a temperature of 28 $^{\circ}$ C. After 5 consecutive screenings, positive transformants were obtained to ensure genetic stability. The GV3101 strain carrying the pSilent-1 served as the control (empty vector) in the ATMT experiment.

4.5. Confirmation of Transformants

Genomic DNA was extracted from *L. qinlingensis* using the Fungal DNA kit (D3390-01; Omega, Norcross, GA, USA) according to the manufacturer's protocol. Using genomic DNA as a template, the primers Hyg-F and Hyg-R were designed for PCR amplification of 1040 bp *Hyg* genes, and the primers Test-F and Test-R were designed on both sides of XhoI and ApaI sites for PCR amplification of 484 bp recombinant fragment (hairpin region) on pSilent-1: LqFlbA.

Total RNA was extracted from *L. qinlingensis* using a UNIQU-10 Column Trizol Total RNA Isolation Kit (B511321; Sangon Biotech, Shanghai, China) according to the protocol provided by the manufacturer. The first-strand cDNA synthesis was initiated using a HiScript[®] III Q RT SuperMix for qPCR (+gDNA wiper; Vazyme, Nanjing, China) transcription kit. To quantify the expression level of the *LqFlbA* gene in the transformants, the primers for FlbA-F and FlbA-R were designed for qRT-PCR using cDNA as the template and the *LqEF1* gene (accession number: AHZ56579.1) as the reference gene. All the reactions were performed with three technical replicates of three biological replicates. The relative expression levels of the genes were computed by the $2^{-\Delta\Delta C_t}$ method of relative quantification [72]. The gene-specific primers of the research are shown in Table 2.

Table 2. Primer sequences used in the research.

Primer Name	Sequences (5'→3')	Purpose
P1 P2	catcgataccgtcgaccGCAGCGAGGATATTTCCAAGAagcttgctggaggatac acgtaagtggatccggGCAGCGAGGATATTTCCAAGAgtagcacaggccttagca	Construction of silencing vectors
Hyg-F Hyg-R	ATGAAAAAGCCTGAACTCAC GGTCGGCATCTACTCTATTC	Confirm transformants
Test-F Test-R	AGGAACGAGGACATTATT GCTGACATCGACACCAAC	Confirm transformants
FlbA-F FlbA-R	GCTATGATCGACACCCTGAAG GTAGTTTCTCAGCGTATGGTCG	qPCR
EF1-F EF1-R	CCGCTGGTACGGGTGAGTT CTTGGTGGTGCCATCTTGTT	qPCR

4.6. Optimization of Transformation Parameters

The evaluated cocultivation parameters that are known to influence transformation frequency included *Agrobacterium* cell concentration (OD₆₀₀ = 0.3, 0.4, 0.5, 0.6, 0.7, and 0.8), conidial suspension concentration (10⁴, 10⁵, 10⁶, 10⁷, and 10⁸ spores/mL), cocultivation time (24, 36, 40, 48, 56, and 64 h), cocultivation temperature (125, 26, 27, 28, 29, and 30 °C), pH of the cocultivation medium (4.4, 4.7, 5.0, 5.3, 5.6, 5.9, and 6.2), and acetosyringone concentration (50, 100, 200, 300, and 400 µM). Based on the preliminary experiments' findings, one parameter was varied while others were kept constant to evaluate each cocultivation condition's effect on transformation. Following cocultivation, the cells were treated with cefotaxime (50 µg/mL) and timentin (150 µg/mL) for 48 h to eliminate *Agrobacterium*. The transformation rate was determined by calculating the number of transformants obtained under different parameter conditions. Each cocultivation parameter was examined in triplicate in at least three independent experiments.

4.7. Growth and Pathogenicity Assay of Transformants

We verified the effect of *FlbA* on the growth of *L. qinlingensis* by measuring the growth rate and colony morphology of the transformants. The three transformants were incubated on the PDA plate containing hygromycin B at 28 °C for 7 days. We drilled holes in the edges of the PDA plate and inoculated fresh mycelia plugs into the center of the new PDA plate. We measured the colony radius and recorded the colony morphology every 5 days under dark cultivation at 28 °C. The transformant carrying the empty vector (*LqFlbA-EV*) served as the control in this experiment. Each treatment was repeated three times.

Fungal inoculation into *P. armandii* stems was modified from the methods in Pham et al. (2014) [73]. Wild-type (WT) and transformant variants with the highest silencing efficiency (*LqFlbA-RNAi-3*) were selected for pine sapling inoculation experiments. We used non-inoculated agar as a control for the inoculation effect. Ten saplings were inoculated with each strain. Holes were drilled with a 0.5 cm cork borer at 4 cm above the soil line. Mycelia plugs of the wild type, transformants, and non-inoculated agar (control) were placed into the holes, and the bark was replaced over the mycelial plugs to close the inoculation holes.

All the holes that were drilled for fungal inoculation were wrapped with cling wrap and sealed with duct tape to avoid contamination. Each treatment was repeated three times with new saplings and fungus for each replicate. The saplings' phloem diseased spot length was measured every 15 days.

4.8. Statistical Analysis

All the data were presented as averages \pm SE. The statistical analysis package SPSS 22.0 (SPSS Inc., Chicago, IL, USA) was used to perform statistical analyses. The one-way ANOVA with Tukey's test was used for multiple comparison analyses. A value of $p < 0.05$ was considered to be statistically significant. The different letters on the graphs indicate significant differences among the treatments. Line charts and histograms were drawn with OriginPro 2021 software (OriginLab, Northampton, MA, USA). PCR products were scanned under the imaging system (ChemiDoc XRS+; Bio-Rad, Hercules, CA, USA). Photos of colonies and lesions were taken by stereomicroscope (DS-R12; Nikon, Tokyo, Japan). The schematic diagram of the vector construction and group diagram was drawn using Adobe Photoshop CS6 (Adobe, San Jose, CA, USA).

Author Contributions: T.G., M.T. and H.C. conceived and designed the experiment; T.G. and H.A. performed the experiments; T.G. performed the data analyses; T.G. wrote the original draft; H.C. reviewed and edited the document. All authors have read and agreed to the published version of the manuscript.

Funding: This research was funded by the National Natural Science Foundation of China, grant number 31870636.

Institutional Review Board Statement: Not applicable.

Informed Consent Statement: Not applicable.

Data Availability Statement: Data is contained within this article.

Acknowledgments: We acknowledge support with respect to the collection of *Leptographium qinlingensis* from Huangguan Forest Farm of Ningxi Forestry Bureau, Xian, China.

Conflicts of Interest: The authors declare no conflict of interest.

References

1. Li, X.J.; Gao, J.M.; Chen, H.; Zhang, A.L.; Tang, M. Toxins from a symbiotic fungus, *Leptographium qinlingensis* associated with *Dendroctonus armandi* and their in vitro toxicities to *Pinus armandi* seedlings. *Eur. J. Plant Pathol.* **2012**, *134*, 239–247. [[CrossRef](#)]
2. Chen, W.Y.; Fan, X.L.; Tian, C.M.; Li, F.; Chou, G.F. Identification and characterization of *Neocosmospora silvicola* causing canker disease on *Pinus armandii* in China. *Plant Dis.* **2023**. [[CrossRef](#)] [[PubMed](#)]
3. Chen, H.; Tang, M. Spatial and temporal dynamics of bark beetles in Chinese white pine in Qinling Mountains of Shaanxi province, China. *Environ. Entomol.* **2014**, *36*, 1124–1130. [[CrossRef](#)]
4. Gan, T.; An, H.L.; Tang, M.; Chen, H. Phylogeny of regulators of G-protein signaling genes in *Leptographium qinlingensis* and expression levels of three RGSs in response to different terpenoids. *Microorganisms* **2022**, *10*, 1698. [[CrossRef](#)]
5. Wang, H.; Wang, T.; Liu, Y.; Zeng, F.; Zhang, H.; Decock, C.; Zhang, X.; Lu, Q. Diversity of Ophiostomatoid fungi associated with *Dendroctonus armandi* infesting *Pinus armandii* in western China. *J. Fungi* **2022**, *8*, 214. [[CrossRef](#)] [[PubMed](#)]
6. Hu, X.; Wang, C.Y.; Wang, L.; Zhang, R.R.; Chen, H. Influence of temperature, pH and metal ions on guaiacol oxidation of purified laccase from *Leptographium qinlingensis*. *World J. Microbiol. Biotechnol.* **2014**, *30*, 1285–1290. [[CrossRef](#)]
7. Bracewell, R.R.; Six, D.L. Broadscale specificity in a bark beetle–fungal symbiosis: A spatio-temporal analysis of the mycangial fungi of the western pine beetle. *Microb. Ecol.* **2014**, *68*, 859–870. [[CrossRef](#)]
8. Dai, L.L.; Li, H.; Zheng, J.; Chen, H. Transcriptome analyses of the Chinese white pine beetle–fungal symbiont *Leptographium qinlingensis* under terpene stress or growth on host pine sawdust. *Symbiosis* **2022**, *86*, 17–31. [[CrossRef](#)]
9. Dohet, L.; Grégoire, J.C.; Berasategui, A.; Kaltenpoth, M.; Biedermann, P.H. Bacterial and fungal symbionts of parasitic *Dendroctonus* bark beetles. *FEMS Microbiol. Ecol.* **2016**, *92*, fiw129. [[CrossRef](#)]
10. Lehenberger, M.; Foh, N.; Göttlein, A.; Six, D.; Biedermann, P.H.W. Nutrient-poor breeding substrates of ambrosia beetles are enriched with biologically important elements. *Front. Microbiol.* **2021**, *12*, 664542. [[CrossRef](#)]
11. Six, D.L. Niche construction theory can link bark beetle–fungus symbiosis type and colonization behavior to large scale causal chain-effects. *Curr. Opin. Insect Sci.* **2020**, *39*, 27–34. [[CrossRef](#)] [[PubMed](#)]

12. Six, D.L.; Elser, J.J. Mutualism is not restricted to tree-killing bark beetles and fungi: The ecological stoichiometry of secondary bark beetles, fungi, and a scavenger. *Ecol. Entomol.* **2020**, *45*, 1134–1145. [[CrossRef](#)]
13. Dai, L.L.; Zheng, J.; Ye, J.Q.; Chen, H. Phylogeny of *Leptographium qinlingensis* cytochrome P450 genes and transcription levels of six CYPs in response to different nutrition media or terpenoids. *Arch. Microbiol.* **2021**, *204*, 16. [[CrossRef](#)] [[PubMed](#)]
14. Dai, L.L.; Li, Z.M.; Yu, J.M.; Ma, M.Y.; Zhang, R.R.; Chen, H.; Pham, T. The CYP51F1 gene of *Leptographium qinlingensis*: Sequence characteristic, phylogeny and transcript levels. *Int. J. Mol. Sci.* **2015**, *16*, 12014–12034. [[CrossRef](#)]
15. An, H.L.; Gan, T.; Tang, M.; Chen, H. Molecular mechanism of overcoming host resistance by the target of rapamycin gene in *Leptographium qinlingensis*. *Microorganisms* **2022**, *10*, 503. [[CrossRef](#)]
16. Shafran, H.; Miyara, I.; Eshed, R.; Prusky, D.; Sherman, A. Development of new tools for studying gene function in fungi based on the Gateway system. *Fungal Genet. Biol.* **2008**, *45*, 1147–1154. [[CrossRef](#)]
17. McDonald, T.; Brown, D.; Keller, N.P.; Hammond, T.M. RNA silencing of mycotoxin production in *Aspergillus* and *Fusarium* species. *Mol. Plant Microbe Interact.* **2005**, *18*, 539–545. [[CrossRef](#)]
18. Nakayashiki, H. RNA silencing in fungi: Mechanisms and applications. *FEBS Lett.* **2005**, *579*, 5950–5957. [[CrossRef](#)]
19. Jeon, J.; Park, S.Y.; Chi, M.H.; Choi, J.; Park, J.; Rho, H.S.; Kim, S.; Goh, J.; Yoo, S.; Choi, J.; et al. Genome-wide functional analysis of pathogenicity genes in the rice blast fungus. *Nat. Genet.* **2007**, *39*, 561–565. [[CrossRef](#)]
20. Bolton, M.D.; van Esse, H.P.; Vossen, J.H.; de Jonge, R.; Stergiopoulos, I.; Stulemeijer, I.J.; van den Berg, G.C.; Borrás-Hidalgo, O.; Dekker, H.L.; de Koster, C.G.; et al. The novel *Cladosporium fulvum* lysin motif effector Ecp6 is a virulence factor with orthologues in other fungal species. *Mol. Microbiol.* **2008**, *69*, 119–136. [[CrossRef](#)]
21. Van Esse, H.P.; Van't Klooster, J.W.; Bolton, M.D.; Yadeta, K.A.; Van Baarlen, P.; Boeren, S.; Vervoort, J.; de Wit, P.J.; Thomma, B.P. The *Cladosporium fulvum* virulence protein Avr2 inhibits host proteases required for basal defense. *Plant Cell* **2008**, *20*, 1948–1963. [[CrossRef](#)]
22. Carneiro, J.S.; de la Bastide, P.Y.; Chabot, M.; Lerch, L.; Hintz, W.E. Suppression of polygalacturonase gene expression in the phytopathogenic fungus *Ophiostoma novo-ulmi* by RNA interference. *Fungal Genet. Biol.* **2010**, *47*, 399–405. [[CrossRef](#)]
23. Kück, U.; Hoff, B. New tools for the genetic manipulation of filamentous fungi. *Appl. Microbiol. Biotechnol.* **2010**, *86*, 51–62. [[CrossRef](#)] [[PubMed](#)]
24. Dong, Y.H.; Wang, S.T. *Agrobacterium tumefaciens*-mediated transformation method for *Fusarium oxysporum*. In *Fusarium Wilt: Methods and Protocols*; Coleman, J., Ed.; Springer: New York, NY, USA, 2022; Volume 2391, pp. 63–73.
25. Michielse, C.B.; Hooykaas, P.J.; van den Hondel, C.A.; Ram, A.F. *Agrobacterium*-mediated transformation as a tool for functional genomics in fungi. *Curr. Genet.* **2005**, *48*, 1–17. [[CrossRef](#)] [[PubMed](#)]
26. Thai, H.D.; Nguyen, B.T.; Nguyen, V.M.; Nguyen, Q.H.; Tran, V.T. Development of a new *Agrobacterium*-mediated transformation system based on a dual auxotrophic approach in the filamentous fungus *Aspergillus oryzae*. *World J. Microbiol. Biotechnol.* **2021**, *37*, 92. [[CrossRef](#)]
27. Thai, H.D.; Do, L.; Nguyen, X.T.; Vu, T.X.; Tran, H.T.T.; Nguyen, H.Q.; Tran, V.T. A newly constructed *Agrobacterium*-mediated transformation system based on the hisB auxotrophic marker for genetic manipulation in *Aspergillus niger*. *Arch. Microbiol.* **2023**, *205*, 183. [[CrossRef](#)] [[PubMed](#)]
28. Lengeler, K.B.; Davidson, R.C.; D'Souza, C.; Harashima, T.; Shen, W.C.; Wang, P.; Pan, X.; Waugh, M.; Heitman, J. Signal transduction cascades regulating fungal development and virulence. *Microbiol. Mol. Biol. Rev.* **2000**, *64*, 746–785. [[CrossRef](#)]
29. Neves, S.R.; Ram, P.T.; Iyengar, R. G protein pathways. *Science* **2002**, *296*, 1636–1639. [[CrossRef](#)] [[PubMed](#)]
30. Yu, J.H. Heterotrimeric G protein signaling and RGSs in *Aspergillus nidulans*. *J. Microbiol.* **2006**, *44*, 145–154.
31. Zhang, H.F.; Tang, W.; Liu, K.Y.; Huang, Q.; Zhang, X.; Yan, X.; Chen, Y.; Wang, J.S.; Qi, Z.Q.; Wang, Z.Y.; et al. Eight RGS and RGS-like proteins orchestrate growth, differentiation, and pathogenicity of *Magnaporthe oryzae*. *PLoS Pathog.* **2011**, *7*, e1002450. [[CrossRef](#)]
32. Shin, K.S.; Park, H.S.; Kim, Y.H.; Yu, J.H. Comparative proteomic analyses reveal that FlbA down-regulates gliT expression and SOD activity in *Aspergillus fumigatus*. *J. Proteom.* **2013**, *87*, 40–52. [[CrossRef](#)]
33. Han, K.-H.; Seo, J.-A.; Yu, J.-H. Regulators of G-protein signalling in *Aspergillus nidulans*: RgsA downregulates stress response and stimulates asexual sporulation through attenuation of GanB (G α) signalling. *Mol. Microbiol.* **2004**, *53*, 529–540. [[CrossRef](#)] [[PubMed](#)]
34. Park, H.-S.; Kim, M.-J.; Yu, J.-H.; Shin, K.-S. Heterotrimeric G-protein signalers and RGSs in *Aspergillus fumigatus*. *Pathogens* **2020**, *9*, 902. [[CrossRef](#)]
35. Xie, R.; Yang, K.; Tumukunde, E.; Guo, Z.; Zhang, B.; Liu, Y.; Zhuang, Z.; Yuan, J.; Wang, S.; Buan, N.R. Regulator of G protein signaling contributes to the development and aflatoxin biosynthesis in *Aspergillus flavus* through the regulation of G α activity. *Appl. Environ. Microbiol.* **2022**, *88*, e00244-22. [[CrossRef](#)] [[PubMed](#)]
36. Lee, B.N.; Adams, T.H. Overexpression of flbA, an early regulator of *Aspergillus* asexual sporulation, leads to activation of brlA and premature initiation of development. *Mol. Microbiol.* **1994**, *14*, 323–334. [[CrossRef](#)]
37. Yan, H.J.; Zhou, Z.H.; Shim, W.B. Two regulators of G-protein signaling (RGS) proteins FlbA1 and FlbA2 differentially regulate fumonisin B1 biosynthesis in *Fusarium verticillioides*. *Curr. Genet.* **2021**, *67*, 305–315. [[CrossRef](#)] [[PubMed](#)]
38. Weld, R.J.; Plummer, K.M.; Carpenter, M.A.; Ridgway, H.J. Approaches to functional genomics in filamentous fungi. *Cell Res.* **2006**, *16*, 31–44. [[CrossRef](#)]

39. Frandsen, R.J. A guide to binary vectors and strategies for targeted genome modification in fungi using *Agrobacterium tumefaciens*-mediated transformation. *J. Microbiol. Methods* **2011**, *87*, 247–262. [[CrossRef](#)]
40. Arenz, C.; Schepers, U. RNA interference: From an ancient mechanism to a state of the art therapeutic application? *Naturwissenschaften* **2003**, *90*, 345–359. [[CrossRef](#)]
41. Cheng, P.; He, Q.; He, Q.; Wang, L.; Liu, Y. Regulation of the *Neurospora circadian* clock by an RNA helicase. *Genes Dev.* **2005**, *19*, 234–241. [[CrossRef](#)]
42. Huang, E.X.; Zhang, Y.; Sun, L.; Zhu, Y.R.; Tang, S.Y.; Mo, C.H.; Zhao, B.Y.; Lu, H. Swnk plays an important role in the biosynthesis of swainsonine in *Metarhizium anisopliae*. *Biotechnol. Lett.* **2023**, *45*, 509–519. [[CrossRef](#)]
43. Flores-Alvarez, L.J.; Corrales-Escobosa, A.R.; Cortés-Penagos, C.; Martínez-Pacheco, M.; Wrobel-Zasada, K.; Wrobel-Kaczmarczyk, K.; Cervantes, C.; Gutiérrez-Corona, F. The *Neurospora crassa* chr-1 gene is up-regulated by chromate and its encoded CHR-1 protein causes chromate sensitivity and chromium accumulation. *Curr. Genet.* **2012**, *58*, 281–290. [[CrossRef](#)] [[PubMed](#)]
44. Scindiya, M.; Malathi, P.; Kaverinathan, K.; Ramesh Sundar, A.; Viswanathan, R. RNA-mediated silencing of PKS1 gene in *Colletotrichum falcatum* causing red rot in sugarcane. *Eur. J. Plant Pathol.* **2019**, *153*, 371–384. [[CrossRef](#)]
45. Scindiya, M.; Malathi, P.; Kaverinathan, K.; Sundar, A.R.; Viswanathan, R. Knock-down of glucose transporter and sucrose non-fermenting gene in the hemibiotrophic fungus *Colletotrichum falcatum* causing sugarcane red rot. *Mol. Biol. Rep.* **2021**, *48*, 2053–2061. [[CrossRef](#)]
46. Bundock, P.; den Dulk-Ras, A.; Beijersbergen, A.; Hooykaas, P.J. Trans-kingdom T-DNA transfer from *Agrobacterium tumefaciens* to *Saccharomyces cerevisiae*. *EMBO J.* **1995**, *14*, 3206–3214. [[CrossRef](#)]
47. De Groot, M.J.A.; Bundock, P.; Hooykaas, P.J.J.; Beijersbergen, A.G.M. *Agrobacterium tumefaciens*-mediated transformation of filamentous fungi. *Nat. Biotechnol.* **1998**, *16*, 839–842. [[CrossRef](#)] [[PubMed](#)]
48. Meyer, V.; Mueller, D.; Strowig, T.; Stahl, U. Comparison of different transformation methods for *Aspergillus giganteus*. *Curr. Genet.* **2003**, *43*, 371–377. [[CrossRef](#)]
49. Sugui, J.A.; Chang, Y.C.; Kwon-Chung, K.J. *Agrobacterium tumefaciens*-mediated transformation of *Aspergillus fumigatus*: An efficient tool for insertional mutagenesis and targeted gene disruption. *Appl. Environ. Microbiol.* **2005**, *71*, 1798–1802. [[CrossRef](#)]
50. Michielse, C.B.; Hooykaas, P.J.; Van den Hondel, C.A.; Ram, A.F. *Agrobacterium*-mediated transformation of the filamentous fungus *Aspergillus awamori*. *Nat. Protoc.* **2008**, *3*, 1671–1678. [[CrossRef](#)] [[PubMed](#)]
51. Wang, Y.; DiGuistini, S.; Wang, T.C.; Bohlmann, J.; Breuil, C. *Agrobacterium*-mediated gene disruption using split-marker in *Grosmannia clavigera*, a mountain pine beetle associated pathogen. *Curr. Genet.* **2010**, *56*, 297–307. [[CrossRef](#)]
52. Hu, Y.F.; Zheng, Y.F.; Liu, B.X.; Gong, Y.X.; Shao, Y.C. Mrhst4 gene, coding for NAD(+)-dependent deacetylase is involved in citrinin production of *Monascus ruber*. *J. Appl. Microbiol.* **2023**, *134*, lxad042. [[CrossRef](#)]
53. Zhang, J.T.; Han, X.G.; Su, Y.; Staehelin, C.; Xu, C.C. T-DNA insertion mutagenesis in *Penicillium brocae* results in identification of an enolase gene mutant impaired in secretion of organic acids and phosphate solubilization. *Microbiology* **2023**, *169*, 001325. [[CrossRef](#)]
54. Idnurm, A.; Bailey, A.M.; Cairns, T.C.; Elliott, C.E.; Foster, G.D.; Ianiri, G.; Jeon, J. A silver bullet in a golden age of functional genomics: The impact of *Agrobacterium*-mediated transformation of fungi. *Fungal Biol. Biotechnol.* **2017**, *4*, 6. [[CrossRef](#)] [[PubMed](#)]
55. Li, D.D.; Tang, Y.; Lin, J.; Cai, W.W. Methods for genetic transformation of filamentous fungi. *Microb. Cell Factories* **2017**, *16*, 168–180. [[CrossRef](#)] [[PubMed](#)]
56. Tanguay, P.; Coupal, J.; Bernier, L. Genetic transformation, electrophoretic karyotyping and isolation of insertional mutants in the tree pathogenic fungus *Neovectria galligena*. *For. Pathol.* **2003**, *33*, 413–428. [[CrossRef](#)]
57. Tanguay, P.; Breuil, C. Transforming the sapstaining fungus *Ophiostoma piceae* with *Agrobacterium tumefaciens*. *Can. J. Microbiol.* **2003**, *49*, 301–304. [[CrossRef](#)] [[PubMed](#)]
58. Royer, J.C.; Dewar, K.; Hubbes, M.; Horgen, P.A. Analysis of a high frequency transformation system for *Ophiostoma ulmi*, the causal agent of Dutch elm disease. *Mol. Gen. Genet. MGG* **1991**, *225*, 168–176. [[CrossRef](#)]
59. Hu, Y.; Dai, Q.Q.; Liu, Y.Y.; Yang, Z.; Song, N.; Gao, X.N.; Voegelé, R.T.; Kang, Z.S.; Huang, L.L. *Agrobacterium tumefaciens*-mediated transformation of the causative agent of valsa canker of apple tree *Valsa mali* var. *mali*. *Curr. Microbiol.* **2014**, *68*, 769–776. [[CrossRef](#)]
60. Foster, A.J.; Morency, M.J.; Séguin, A.; Tanguay, P. *Agrobacterium tumefaciens*-mediated transformation for targeted disruption and over expression of genes in the poplar pathogen *Sphaerulina musiva*. *For. Pathol.* **2014**, *44*, 233–241. [[CrossRef](#)]
61. Mahyudin, M.M.; Foster, G.D.; Bailey, A.M. Optimising *Agrobacterium*-mediated transformation of *Corynespora cassiicola* to deliver DsRed. *J. Rubber Res.* **2020**, *23*, 139–149. [[CrossRef](#)]
62. Rodríguez-Pires, S.; Espeso, E.A.; Baró-Montel, N.; Torres, R.; Melgarejo, P.; De Cal, A. Labeling of *Monilinia fructicola* with GFP and its validation for studies on host-pathogen interactions in stone and pome fruit. *Genes* **2019**, *10*, 1033. [[CrossRef](#)] [[PubMed](#)]
63. McDougal, R.; Yang, S.Y.; Schwelm, A.; Stewart, A.; Bradshaw, R. A novel GFP-based approach for screening biocontrol microorganisms in vitro against *Dothistroma septosporum*. *J. Microbiol. Methods* **2011**, *87*, 32–37. [[CrossRef](#)] [[PubMed](#)]
64. Zhou, Y.H.; Lu, D.D.; Joseph, R.; Li, T.; Keyhani, N.O. High efficiency transformation and mutant screening of the laurel wilt pathogen, *Raffaelea lauricola*. *Appl. Microbiol. Biotechnol.* **2020**, *104*, 7331–7343. [[CrossRef](#)]
65. Lafon, A.; Han, K.H.; Seo, J.A.; Yu, J.H.; d'Enfert, C. G-protein and cAMP-mediated signaling in *aspergilli*: A genomic perspective. *Fungal Genet. Biol.* **2006**, *43*, 490–502. [[CrossRef](#)] [[PubMed](#)]
66. Li, L.; Wright, S.J.; Krystofova, S.; Park, G.; Borkovich, K.A. Heterotrimeric G-protein signaling in filamentous fungi. *Annu. Rev. Microbiol.* **2007**, *61*, 423–452. [[CrossRef](#)]

67. Hicks, J.K.; Yu, J.H.; Keller, N.P.; Adams, T.H. *Aspergillus* sporulation and mycotoxin production both require inactivation of the FadA G alpha protein-dependent signaling pathway. *EMBO J.* **1997**, *16*, 4916–4923. [[CrossRef](#)]
68. Adams, T.H.; Yu, J.H. Coordinate control of secondary metabolite production and asexual sporulation in *Aspergillus nidulans*. *Curr. Opin. Microbiol.* **1998**, *1*, 674–677. [[CrossRef](#)]
69. Yu, J.H.; Rosén, S.; Adams, T.H. Extragenic suppressors of loss-of-function mutations in the *Aspergillus* FlbA regulator of G-protein signaling domain protein. *Genetics* **1999**, *151*, 97–105. [[CrossRef](#)]
70. Li, J.X.; Hong, N.; Peng, B.; Wu, H.J.; Gu, Q.S. Transformation of *Corynespora cassiicola* by *Agrobacterium tumefaciens*. *Fungal Biol.* **2019**, *123*, 669–675. [[CrossRef](#)]
71. Zhong, S.; Leng, Y.; Bolton, M.D. Construction of hairpin RNA-expressing vectors for RNA-mediated gene silencing in fungi. *Methods Mol. Biol.* **2012**, *835*, 623–633. [[CrossRef](#)]
72. Livak, K.J.; Schmittgen, T.D. Analysis of relative gene expression data using real-time quantitative PCR and the 2^{(-Delta Delta C(T))} Method. *Methods* **2001**, *25*, 402–408. [[CrossRef](#)] [[PubMed](#)]
73. Pham, T.; Chen, H.; Yu, J.M.; Dai, L.L.; Zhang, R.R.; Vu, T.Q. The differential effects of the blue-stain fungus *Leptographium qinlingensis* on monoterpenes and sesquiterpenes in the stem of Chinese white pine (*Pinus armandi*) saplings. *Forests* **2014**, *5*, 2730–2749. [[CrossRef](#)]

Disclaimer/Publisher’s Note: The statements, opinions and data contained in all publications are solely those of the individual author(s) and contributor(s) and not of MDPI and/or the editor(s). MDPI and/or the editor(s) disclaim responsibility for any injury to people or property resulting from any ideas, methods, instructions or products referred to in the content.